# Bacteriophage infection drives loss of β-lactam resistance in methicillin-resistant *Staphylococcus aureus*

My Tran*, Angel J. Hernandez Viera*, Patricia Q. Tran, Charlie Y. Mo
Department of Bacteriology, University of Wisconsin-Madison, USA
*Denotes equal contribution
Correspondence: cymo@wisc.edu

**Abstract**

Bacteriophage (phage) therapy has been proposed as a means to combat drug-resistant bacterial pathogens. Infection by phage can select for mutations in bacterial populations that confer resistance against phage infection. However, resistance against phage can yield evolutionary trade-offs of biomedical use. Here we report the discovery of staphylococcal phages that cause different strains of methicillin-resistant *Staphylococcus aureus* (MRSA) to become sensitized to β-lactams, a class of antibiotics against which MRSA is typically highly resistant. MRSA cells that survive infection by these phages display significant reductions in minimal inhibitory concentration against different β-lactams compared to uninfected bacteria. Phage-treated MRSA further exhibited attenuated virulence phenotypes in the form of reduced hemolysis and clumping. Sequencing analysis revealed that the different MRSA strains evolved unique genetic profiles during infection. These results suggest complex evolutionary trajectories in MRSA during phage predation and open up new possibilities to reduce drug resistance and virulence in MRSA infections.

*Staphylococcus aureus* is a Gram-positive bacterium found on the skin and mucosa of humans and animals. It causes a wide range of human diseases, from endocarditis to pneumonia.[1] Methicillin-resistant *S. aureus* (MRSA) is a form of *S. aureus* that displays high levels of drug resistance towards β-lactam antibiotics, such as penicillins and cephalosporins. β-lactams act by inhibiting the activity of transpeptidase enzymes during peptidoglycan synthesis in bacterial cell walls.[2] β-lactams are one of the most commonly prescribed drug classes, and many are designated as "Critically Important" antimicrobials by the World Health Organization.[3]

A chief mediator of β-lactams resistance in MRSA is the SCCmec cassette, a mobile genetic element that carries the resistance gene *mecA.* MecA encodes for the penicillin-binding protein 2A (PBP2a), a transpeptidase that has a low affinity for β-lactams.[4] This lower affinity permits PBP2a to participate in peptidoglycan synthesis even in the presence of β-lactams, ultimately resulting in cell survival. In addition to *mecA*, numerous MRSA strains carry β-lactamases, such as BlaZ, that degrade β-lactams, thus further contributing to drug resistance. MRSA infections pose a considerable public health risk as they are notoriously difficult to treat and are widespread in communities and hospital settings. In 2019, MRSA alone accounted for more than 100,000 deaths attributable to drug-resistant infections worldwide.[5] Developing novel solutions to combat MRSA is a major focus in academia and industry.

Bacteriophages (phages) are viruses that infect and kill bacteria, posing one of the greatest existential threats to bacterial communities. Some estimates suggest that 40% of all bacterial mortality worldwide is caused by phage predation.[6] Due to this lethality, phage therapy has been proposed as an attractive alternative for combating drug-resistant bacterial infections. In phage therapy, lytic phages are administered to kill the bacterial pathogen(s) causing an infection. Phages offer certain advantages over traditional antibiotics: they are highly specific for their hosts by reducing off-target killing; they self-amplify and evolve, enabling the rapid generation of new phage variants with improved activities; and they are generally regarded as safe, based on extremely rare cases of toxicity in animals and patients.[7] Indeed, against staphylococcal infections, over a dozen promising case studies and clinical trials have been reported in the past decade.[8]

Despite these advances, routine use of phage therapy is still met with challenges. Chief among these challenges is the inevitable rise of phage resistance as phage predation exerts a strong selective pressure on bacterial populations. According to one analysis that focused on phage therapy outcomes, resistance against phage evolved in 75 percent of human clinical cases in which the evolution of resistance was monitored.[9] Mutations represent a chief pathway by which bacteria evolve resistance against phage. To date, the best characterized phage resistance mutations strains involve alterations of the cell surface that affect phage attachment. For most lytic phages, the first step of their infection involves attachment of the phage particle to a receptor molecule (or multiple molecules) on the cell surface; these receptors are often proteins or sugar moieties, which are recognized by phage proteins.[8,10,11] Mutations in these receptor molecules can prevent phage binding, leading to resistance. For example, in *Escherichia coli*, mutations in the cell-wall protein LamB confer resistance against lambda phage infection, while in *S. aureus*, mutations that modify the glycopolymers in the cell wall, such as wall teichoic acid (WTA), have been shown to limit the infection by phages.[11,12] Complicating the picture, studies have revealed that a plethora of additional host mechanisms, including

dedicated anti-phage defense systems, can impact the evolution of resistance against phage.[13,14] These problems highlight the importance of developing phage treatment strategies that minimize or capitalize on the evolution of phage resistance.[15]

A unique aspect of phage therapy is the possibility to exploit evolutionary trade-offs to combat resistant pathogens. A genetic trade-off is defined as an evolved trait that confers a fitness advantage against a particular selective pressure at the expense of reduced fitness against an unselected pressure. Across many different species of bacteria, such fitness trade-offs are known to occur between phage resistance and antibiotic resistance (Figure 1A). For example, selection by a lytic phage $PYO^{Sa}$ on the methicillin-sensitive *S. aureus* Newman selected for mutations in the *femA* aminoacyltransferase, leading to increased resistance against phage infection but reduced resistance towards antibiotics.[16] These studies raise the question of whether such phage/antibiotic resistance trade-offs can be induced in actual MRSA strains, which would have significant therapeutic implications. Employing phages to drive the evolution of such beneficial trade-offs could serve as a means to reduce drug resistance. However, very little is known about how frequently these trade-offs occur in different bacterial species, or through what molecular mechanisms they work.

Here we investigate how infection by staphylococcal phages causes three different MRSA strains to evolve sensitivity to different types of β-lactam antibiotics. Interestingly, despite being treated by the same phage, the loss of resistance phenotype is mediated by mutations distinct to each MRSA strain. In addition to resistance, phage infection also causes a reduction in hemolysis and clumping, which are key virulence phenotypes in MRSA. Finally, we isolated a mutant version of the phage that displays enhanced killing, improved resistance reduction, and reduced virulence phenotypes across all three MRSA strains.

## Results

### Identification of ΦStaph1N with activity against multiple MRSA strains

We subjected three MRSA strains – MRSA252 (USA200), MW2 (USA400), and LAC (USA300) – to a panel of staphylococcal phages using plaquing assays (Table S1, Figure S1). All three MRSA strains are pathogenic isolates that have been implicated in human infection and disease and have been used as representative examples for studying MRSA.[17–19] Of the phages tested, one phage, ΦStaph1N, was able to form distinct plaques on all three MRSA strains (Figure 1B). ΦStaph1N belongs to the myovirus family of lytic staphylococcal phages, with a genome size of ~138 kB.[20,21]

Despite its ability to infect all three MRSA strains, ΦStaph1N infection was often unable to effectively lyse MRSA cultures. For example, both MW2 and LAC displayed incomplete lysis in liquid culture at multiplicities of infection (MOIs) of 0.1 or lower (Figure S2). At an MOI of 0.1, we observed that all three MRSA strains lysed within 2-3 hours following phage infection but recovered high cell density after passaging one percent of the culture into fresh media. We therefore hypothesized that predation by ΦStaph1N selected for mutations conferred resistance against ΦStaph1N infection, allowing the culture to regrow. Indeed, ΦStaph1N was unable to form plaques on recovered MRSA cultures that survived in the initial ΦStaph1N infection (Figure 1B).

Next, we asked whether phage resistance against ΦStaph1N infection could cause a trade-off in drug resistance in MRSA. Since both phage and β-lactams interface with

the bacterial cell wall, we hypothesized that phage resistance mutations could impact β-lactam activity. Parental strains of MRSA252, MW2, and LAC displayed higher minimal inhibitory concentrations (MICs) of ≥48 μg/mL against the β-lactams oxacillin (OXA), cefazolin (CEF), amoxicillin (AMX), and amoxicillin & clavulanic acid (AMX+CA), visually indicated by their ability to form lawns surrounding antibiotic strips (Figure 1C, Table S2). The MRSA strains were sensitive to vancomycin (VANC; MICs = 1.5 μg/mL), which inhibits cell wall synthesis through a different mechanism than β-lactams.

By contrast, all strains that survived ΦStaph1N infection displayed a reduction in resistance against OXA, CEF, and AMX+CA, with fold reductions in MIC between 10 and 1000-fold (Figure 1D). No changes in MIC were observed with VANC. These observations suggest that the loss of resistance might be specific to the mechanism of action of β-lactams. Furthermore, phage-treated strains remained resistant to AMX alone, likely caused by the activity of β-lactamases present in the three MRSA strains. Together, these results suggest that predation by ΦStaph1N causes three different MRSA strains to lose their resistance towards β-lactams.

Next, we asked how infection at lower MOIs with ΦStaph1N affected β-lactam resistance in MRSA. We infected the three MRSA strains with ΦStaph1N at MOIs ranging from 0.01 to $10^{-5}$, isolated the surviving MRSA cells, and tested the survivors for their MIC against oxacillin; each condition was tested in three independent replicates (Table S2). For MRSA252, we observed a ~3-order of magnitude fold reduction of MIC in the surviving cells at an MOI of $10^{-5}$. With MW2, the reduction of MIC markedly decreased with lower phage levels, showing on average no reduction in MIC at MOIs of $10^{-3}$ or lower (Table S2). For LAC, two of the replicates displayed an order of magnitude reduction of MIC at an MOI of $10^{-4}$, while one replicate did show a strong decrease in MIC at the same MOI. These results suggest that for MRSA252, MOIs as low as $10^{-5}$ of ΦStaph1N infection can still drive the loss of resistance, while for MW2 and LAC, higher MOIs of phage are needed to ensure the same outcome of reduced β-lactam resistance.

We then asked whether the reduction in β-lactam can be achieved with a phage from a different taxonomical group. The MRSA LAC strain is sensitive to infection by ΦNM1γ6, a lytic version of the temperate phage ΦNM1, displaying plaquing comparable to ΦStaph1N (Table S1, Figure S1). ΦNM1γ6 belongs to the siphovirus family and was derived from the *S. aureus* Newman strain.[22–24] We therefore examined whether infection with ΦNM1γ6 could also reduce β-lactam resistance in LAC. We infected LAC with ΦNM1γ6 at an MOI of 0.1 and measured the MIC against oxacillin of the surviving cells. Here, recovered LAC cultures did not show a reduction in MICs (Figure S3). This suggests that ΦNM1γ6 is unable to reduce resistance in susceptible MRSA hosts, raising the possibility that different phages vary in their ability to change β-lactam resistance in MRSA.

**Discovery of mutant in ΦStaph1N with enhanced activity against MRSA**

A key advantage of phage therapy over conventional pharmaceutical antibiotics is that phages themselves can evolve. For ΦStaph1N, we noticed that while the phage was able to plaque all three MRSA strains, its plaque-forming efficiency was reduced on the MW2 and LAC strains (Figure 1B, Figure S1). ΦStaph1N plaques on MW2 and LAC strains were hazy and the overall efficiency of plaquing was approximately two orders of magnitude less than that with MRSA252. Unexpectedly, we consistently observed

161 smaller, clear plaques arising in the larger, hazy plaques of LAC (Figure 2A). This led us
162 to hypothesize that these clear plaques are caused by a mutant ΦStaph1N that plaques
163 more efficiently on LAC. We therefore isolated phage clones from these single plaques
164 and tested for their activity against MRSA. This mutant phage, which we called Evo2, is
165 able to plaque on LAC and MW2 strains with higher efficiency, displaying comparable
166 plaquing to MRSA252 (Figure 2A, Figure S1). In growth curve experiments, we further
167 observed that Evo2 lyses MRSA cultures at lower MOIs compared to ΦStaph1N (Figure
168 S2). Notably, Evo2 exhibits lytic activity against MW2 and LAC even at an MOI of 0.0001,
169 a concentration at which ΦStaph1N does not show any detectable activity against the two
170 strains.
171 We sequenced the genome of Evo2 to determine the genetic mechanism driving
172 this enhanced activity. We observed a single point mutation in ORF141 that induces a
173 premature stop codon (Figure S4). Sequence analysis with HHpred predicts ORF141 to
174 be a putative DNA binding protein with an HTH motif (PDB: 2LVS, E-value: 2.5e-9). We
175 speculate that this protein is a transcriptional regulator that when inactivated by a
176 nonsense mutation, increases ΦStaph1N infectivity. Future studies will center on
177 determining the mechanism of this mutation and why Evo2 only evolved in the LAC strain.
178 Given Evo2's enhanced activity against MRSA, we then asked how predation by
179 Evo2 impacted β-lactam resistance in our three MRSA strains. We infected MRSA252,
180 MW2, and LAC with Evo2 at an MOI of 0.1 and measured the MICs against β-lactams
181 after 48 hours of passaging. Broadly, similar to the ΦStaph1N infection, infection by Evo2
182 reduced the MICs of the three MRSA strains against OXA, CEF, and AMX+CA, while
183 MICs against AMX alone and VAN did not change significantly (Figure 2B).
184 We then tested how different MOIs of Evo2 impacted β-lactam resistance in MRSA
185 (Table S2). As with ΦStaph1N, we infected the three MRSA strains with Evo2 at varying
186 MOIs from $10^{-2}$ to $10^{-5}$ and measured the MIC against oxacillin in the evolved MRSA;
187 each condition was tested in three independent replicates. For most of the MRSA252
188 cultures, we did not see a significant difference in the fold reduction of MIC between
189 ΦStaph1N and Evo2. Across all three strains, we observed that replicate cultures across
190 different MOIs were unable to recover growth following Evo2 infection (Table S2).
191 However, cultures of MW2 and LAC that did regrow displayed a loss of oxacillin
192 resistance. Thus, overall Evo2 displays a higher infectivity against the three MRSA strains
193 and a greater potency in reducing β-lactam resistance.
194
195 **Genomic mutations in MRSA strains following phage infection**
196 Following these MIC tests, we hypothesized that the phage-treated MRSA stains
197 evolved mutations that increased their sensitivity to β-lactams. We sequenced the
198 genomes of three clonal isolates (A-C) from each MRSA strain that underwent ΦStaph1N,
199 Evo2, or a mock infection. We observed that each MRSA strain evolved distinct mutation
200 profiles (Figure 3A). Irrespective of the strain and phage treatment, most mutations were
201 predicted to result in substitutions in the protein product, followed by truncations (Figure
202 S5). Cluster of Orthologous Genes (COG) variants associated with transcription, cell
203 wall/membrane/envelope biogenesis, coenzyme transport and metabolism, and defense
204 mechanisms, were the most commonly found categories. Mutations in annotated genes
205 that appeared at least twice across the clonal replicates are summarized in Table 1.
206 Information on all detected genetic variants is listed in Supplementary Table 1.

207 **Table 1. Mutated genes in MRSA following infection with phages ΦStaph1N or Evo2**

| Gene | Description | Strain | Phage infection | Reference |
|---|---|---|---|---|
| *sarA* | Transcriptional regulator of antibiotic resistance and virulence | MW2 | Evo2 | [25,26] |
| *mgrA* | Transcriptional regulator of antibiotic resistance and virulence | MW2 | ΦStaph1N, Evo2 | [27,28] |
| *rpoB* | Transcriptional regulator of antibiotic resistance | LAC | ΦStaph1N, Evo2 | [29] |
| *arlR* | Transcriptional regulator of antibiotic resistance and virulence | LAC | ΦStaph1N, Evo2 | [28,30,31] |
| *spoVG* | Transcriptional regulator of antibiotic resistance and virulence | LAC | ΦStaph1N, Evo2 | [32,33] |
| *cysE* | Cysteine and methionine synthesis, serine O-acetyltransferase | MW2 | Evo2 | [34] |
| *metK* | Cysteine and methionine synthesis, S-adenosylmethionine (SAM) synthetase | MW2 | ΦStaph1N, Evo2 | [35] |
| *trpF* | Phenylalanine, tyrosine and tryptophan synthesis, phosphoribosylanthranilate isomerase | LAC | ΦStaph1N, Evo2 | [36] |
| *femA* | Peptidoglycan synthesis, pentaglycine synthesis | MRSA252 | ΦStaph1N, Evo2 | [37,38] |
| *murE* | Peptidoglycan synthesis, UDP-MurNAc tripeptide synthesis | MW2 | ΦStaph1N, Evo2 | [39] |
| *trpS* | Aminoacyl-tRNA synthesis, tryptophanyl-tRNA synthesis | MW2 | ΦStaph1N, Evo2 | |
| *ytqA* | tRNA modifications, $mnm^5s^2U$ synthesis | MW2 | ΦStaph1N, Evo2 | [40] |
| *yvcD* | Unknown | MW2 | Evo2 | |
| *natA* | ABC transporter | MW2 | ΦStaph1N, Evo2 | [41] |
| *tcaB* | Predicted multidrug efflux pump | MW2 | ΦStaph1N, Evo2 | [42] |

208

209 In all MRSA strains, we found mutations that could account for the loss in β-lactam
210 resistance. In MRSA252, both ΦStaph1N and Evo2 infection were selected for frameshift
211 or nonsense mutations in the *femA* gene that would inactive the protein product. FemA is
212 required for the synthesis of the pentaglycine branch on *S. aureus* Lipid II, the
213 peptidoglycan precursor (Table 1). Deletions of *femA* have been shown to increase
214 susceptibility to β-lactams even when PBP2a (encoded by *mecA*) is expressed.[37,38] These
215 results thus provide a potential mechanism for how some MRSA252 cells lose β-lactam
216 resistance after phage selection. At the same time, we noted the presence of other
217 uncharacterized mutations in phage-treated MRSA252. For example, clone A of
218 ΦStaph1N-treated cells carried 2 mutations: a frameshift in *femA* and a substitution
219 mutation in an uncharacterized protein; meanwhile, clone B displayed a substitution
220 mutation in *pfkA*, a predicted ATP-dependent 6-phosphofructokinase and mutation in an
221 intergenic region; clone C showed a substitution mutation in a putative transport protein,
222 called *yueF* (Figure 3B, Supplementary Table 1). The role of these mutations in mediating
223 phage resistance or β-lactam sensitivity, if any, remains unknown.
224 In MW2, we found mutations in two transcriptional regulators, *mgrA* and *sarA*
225 (Figure 3A, Table 1). Both *mgrA* and *sarA* belong to the family of MarR (multiple antibiotic
226 resistance regulator)/SarA (staphylococcal accessory regulator A) proteins, which
227 regulate drug resistance and virulence in *S. aureus*.[25–27] In ΦStaph1N-treated MW2, only
228 *mgrA* was mutated, while in Evo2-treated MW2, clones also showed nonsense mutations
229 in *sarA.* We also found mutations in *metK* and *ytqA* which are both predicted to be
230 associated with S-adenosylmethione: *metK* synthesizes SAM, while *ytqA* belongs to the
231 radical SAM enzyme family and is predicted to be involved in tRNA modification.[35,40]
232 Phage-treated MW2 also displayed mutations in other genes, including *tcaB and murE*.

233 Notably, each clonal replicate had multiple mutations in the genome, while by contrast
234 untreated MW2 cells only displayed a deletion in an intergenic region that is not present
235 in any of the phage-treated samples.
236 In the LAC strain, we observed a third, distinct mutational pattern (Figure 3A). Of
237 note, we found nonsense mutations in *arlR,* which is part of the *arlRS* two-component
238 signaling system (Table 1). The activity of ArlRS has been implicated in *S. aureus*
239 virulence, pathogenicity, and oxacillin resistance.[30,31] Further, we observed substitution
240 mutations in *spoVG*, which is a transcription factor regulating the expression genes
241 involved in a variety of functions, including cell wall metabolism (Table 1).[32] Indeed,
242 SpoVG activates the expression of *femA*.[33] Studies have shown that SpoVG modulates
243 β-lactam antibiotic resistance by modulating cell wall synthesis.[33] Similar to the other two
244 MRSA strains, phage-treated clones of LAC showed multiple mutations in their genomes,
245 although their association with β-lactam sensitivity remains unclear. Finally, we observed
246 mutations in *prsA* and *bioA* that appeared in both the mock and phage treatment
247 conditions, suggesting that these mutations do not arise due to phage selection.
248
249 **Phage-treated MRSA strains display reduced virulence phenotypes**
250 *S. aureus* strains encode a wide variety of virulence factors that facilitate bacterial
251 infection, and previous studies have used MW2 and LAC strains as models of MRSA
252 virulence.[27,28] In MW2 and LAC, we observed the evolution of nonsense mutations in
253 known virulence regulators, such as *mgrA*, *arlR*, and *sarA*. We therefore hypothesized
254 that phage-treated MRSA cells could also display altered virulence phenotypes in addition
255 to reduced β-lactam resistance. We first tested the ability of MRSA strains that survived
256 phage predation for their ability to form biofilms in a Crystal Violet assay. We found that
257 Evo2 infection of MRSA252 resulted in a significant reduction in Crystal Violet absorption
258 compared to the parental strain. However, we show no significant difference in Crystal
259 Violet absorption between parental, mock- and phage-treated MW2 and LAC strains
260 (Figure S6).
261 Next, we tested whether phage infection could affect the hemolysis of rabbit blood
262 cells. Hemolysis is mediated by the secretion of toxins, such as alpha toxins, and plays
263 an important role in MRSA infection.[43] Expression of these toxins is regulated by virulence
264 pathways that comprise numerous transcription factors, including *mgrA*, *arlR*, and *sarA.*
265 Parental MW2 and LAC colonies lysed rabbit blood cells on blood agar plates, producing
266 distinct halos of clearance around the bacterial cells. As expected, for untreated LAC, the
267 total area of hemolysis was on average 3-fold larger than that of untreated MW2 (~210
268 $mm^2$ vs ~70 $mm^2$, respectively); with MRSA252, by contrast, lysis was not detected
269 (Figure 4A). Following treatment with ΦStaph1N, we observed that MW2 and LAC
270 displayed a reduced area of hemolysis by 4 to 5-fold. With Evo2-treated cells, we found
271 that in MW2 the fold reduction was comparable to that of ΦStaph1N-treated cells.
272 However, for Evo2-treated LAC, loss of hemolysis was even more pronounced, with two
273 of the replicates showing no detectable hemolysis.
274 *S. aureus* is also able to bind to fibrinogen, resulting in the agglutination, or
275 clumping, of bacteria. Clumping is thought to have several functions in the context of
276 staphylococcal infections. Clumps are likely to be more resistant to clearance by the
277 immune system, partly because they may be too large to be phagocytosed by
278 neutrophils.[28] Similar to the expression of hemolysins, previous work has shown that

clumping in MW2 and LAC is regulated by a network of virulence regulators. For MW2 and LAC, we observed that phage-treated cells displayed less clumping than the mock-treated or parental strain. For MW2, ΦStaph1N infection resulted in a modest reduction, while Evo2 infection resulted in a reduction of approximately 3-fold (Figure 4B). In LAC, we found that both ΦStaph1N and Evo2 treatment resulted in comparable reductions of clumping in surviving cells.

## Discussion

Here we report the discovery that infection by the myovirus ΦStaph1N and its derivative Evo2 can drive MRSA populations to evolve favorable genetic trade-offs between phage and β-lactam resistance. MRSA strains that survived phage infection were resistant to phage; however, they displayed up to a 1000-fold decrease in their MICs against β-lactam antibiotics. Sequencing revealed that each of the three MRSA strains tested evolved distinct mutational profiles following phage infection. Of these mutations, a significant portion of the affected genes are involved in transcriptional regulation, antibiotic resistance, and cell maintenance. Concurring with the sequencing data, phage-treated MRSA strains displayed attenuated virulence phenotypes in the form of reduced hemolysis and cellular agglutination.

Our system highlights the multitude of evolutionary paths that different bacterial strains can undertake to evolve resistance against phage. Most staphylococcal phages are thought to adsorb to *S. aureus* by recognizing wall teichoic acid (WTA). Prior work has revealed that phage resistance in *S. aureus* can arise from the disruption of genes involved in the synthesis and modification of WTA, such as *tagO or tarM*.[44] Some MRSA strains also alter cell wall glycosylation through dedicated genes encoded on prophages.[11] Additionally, the presence of cell wall-bound Protein A has been shown to decrease phage absorption, likely by masking WTA.[45] However, our results suggest that the evolution of phage resistance can potentially impact networks of genes in the different MRSA strains, including metabolic genes and transcription factors. For example, both *mgrA* and *arlRS* regulate the expression of proteins associated with the cell wall, such as the Giant Staphylococcal Surface Protein (GSSP).[28] We hypothesize that mutations in these regulators might perturb the composition of proteins in the cell wall, which in turn can disrupt phage binding or prevent disrupt injection of the phage nucleic acid into the cytoplasm. Further studies are needed to dissect the effect of these gene networks on phage resistance and β-lactam resistance.

Our study also shows some of the challenges associated with determining phage/antibiotic resistance trade-offs. Not only do different bacterial strains evolve distinct mutations, but individual clones can accumulate multiple mutations in their genome. Such complex dynamics have been observed in other coevolving bacteria-phage systems before and can serve as useful models to study evolution. However, they make it difficult to predict broader phenotypic outcomes in the bacteria following phage infection. For example, phage resistance has also been shown to confer so-called “trade-ups,” where a non-selected trait is enhanced (e.g. cross-resistance between phage and antibiotic). In our study, we cannot rule out that our phage-treated MRSA has evolved (or will evolve) trade-ups. Although further research is required to test this possibility, the potential clinical benefit of reduced resistance and virulence in MRSA may outweigh the risks associated with trade-ups.

Despite evolving distinct mutational profiles, the three MRSA strains nonetheless displayed a convergence of phenotypes in the form of enhanced phage resistance, reduced β-lactam resistance, and attenuated virulence. We posit that this convergence is caused by the involvement of the cell wall in all three phenotypic outcomes. Phages must interface with the cell wall to adsorb, β-lactams target proteins associated with the maintenance of the cell wall, and many *S. aureus* virulence factors are embedded within the cell wall or need to get secreted through it. The integrity and composition of the cell wall can be determined by numerous genes, ranging from single proteins involved in cell wall synthesis, such as *femA*, to transcriptional regulators that control the expression of cell wall-associated proteins, such as *mgrA*. Thus, the mutational patterns observed in each MRSA strain might reflect unique genetic solutions that enable the bacteria to adapt to the phage predation, while also maximizing the fitness for that particular strain.

From a biomedical perspective, exploiting phage/antibiotic resistance trade-offs have been proposed as a means to combat resistance in bacterial pathogens.[15] Not only could phage treatments reduce the bacterial load of an infection, but also potentially resensitize the bacterial population to antibiotics that it was previously resistant against. For example, in our study, we observed that the MIC of phage-treated MRSA against oxacillin dropped below 2 μg/mL, which is designated by the FDA as the oxacillin MIC susceptible breakpoint for *S. aureus*. We speculate that infection by ΦStaph1N, Evo2, or an equivalent phage can facilitate the re-deployment of β-lactams in the treatment against MRSA infections. Additionally, phage-treated MRSA might also lose virulence and become more susceptible to immune clearance, which can further improve treatment outcomes. Future studies will need to examine this hypothesis in animal infection models.

**Acknowledgments**

MT is supported by the SciMed GRS program at UW-Madison; CYM is supported by start-up funds from the Department of Bacteriology at UW-Madison. We are grateful to Dr. Wilmara Salgado-Pabón for providing us with MRSA strains and helpful suggestions. We thank the Marraffini and Hatoum-Aslan laboratories for providing us with bacteriophage samples. We also thank all members of the Mo lab for their scientific input.

## Online Methods

### Strains and culture conditions

The bacterial strains used in this study are listed in Table S1. Unless otherwise indicated, all MRSA strains (LAC, MRSA252, MW2) were grown in Brain Heart Infusion (BHI) media at 37 ºC with shaking (235 RPM).

### Plate-based plaque assay

Bacterial lawns were prepared by mixing 100 μL of an overnight culture with 5 mL of melted BHI agarose (top agar). The bacteria and top agar mixture were poured onto a solid BHI plate. The plate was dried for 10 minutes. 10-fold serial dilutions ($10^0$ -$10^{-7}$ unless otherwise noted) of phage were then spotted on the bacterial lawn. Plates were then incubated at 37 ºC for 16 hours. Phage titer in plaque-forming units per μL (pfu/μL) was then calculated.

### Phage infection assay

371 MRSA strains were plated onto BHI agar plates and grown overnight. Individual colonies
372 from the parental strains (also referred to as P0) were picked. Single colonies were
373 inoculated in a round bottle tube containing 5 mL BHI broth. The cultures were incubated
374 at 37 ºC, 235 RPM for 24 hours. The grown P0 cultures were then diluted 1:100 into fresh
375 5 mL BHI broth. At the early log phase (OD ~0.3), the bacterial cultures were treated with
376 phage at an MOI of 0.1, unless indicated otherwise. The treated bacterial cultures were
377 incubated at 37 ºC with shaking (235 RPM) for 24 hours. The cultures were then
378 passaged 1:100 into fresh 5 mL BHI broth. This passage was then grown at 37 ºC, 235
379 RPM, for another 24 hours. Surviving cultures were then used for both phenotypic assays
380 and sequencing experiments. As a negative control, MRSA strains were passaged using
381 the steps described above without phage treatment (mock).
382
383 **MIC assay**
384 Bacterial lawns were normalized to contain $1x10^8$ CFU/mL bacteria mixed with top agar
385 for a total volume of 5 mL. The bacteria and top agar mixture is poured onto a solid BHI
386 plate. The plate was dried for 10 minutes. MIC with increasing concentrations of
387 antibiotics were placed on the semi-dried bacterial lawn and allowed to dry for 10 minutes.
388 The plates are then incubated at 37 ºC overnight. For analysis, the plates were imaged,
389 and the MIC of the bacteria was determined. The MIC is determined at the edge of the
390 inhibition ellipse intersects the side of the strip.
391
392 **Rabbit blood hemolysis**
393 Phage-treated or mock-treated cultures were diluted to an OD600 of 0.1, 5 µL of this
394 dilution was spotted on rabbit blood TSB agar plates and incubated at 37 ºC for 24 hours.
395 The area of clearance was determined by the following formula:
396 $[\pi\ (\text{diameter of clearance}/2)^2] - [\pi(\text{diameter of bacterial spot}/2)^2]$
397
398 **Clumping assay**
399 Clumping assays were performed as described previously.[46] In short, overnight cultures
400 were diluted 1:100 and incubated at 37 ℃ until the cultures reached an $OD_{600}$ of 1.5. At
401 this point, 1.5 mL of culture was washed two times and resuspended with PBS.
402 Lyophilized human plasma was added for a final concentration of 1.25%. Resuspended
403 cells were left to sit statically at room temperature. 100uL were taken from the top of the
404 cell suspensions in 30-minute intervals and the $OD_{600}$ was measured.
405
406 **Biofilm assay**
407 Biofilm assay was performed using the crystal violet method as outlined.[47] In brief,
408 overnight cultures grown in BHI at 37 ºC were back diluted 1:10 into a 96-well bottomed
409 microwell plate. The plates were incubated at 37 ºC overnight. The contents in the plate
410 were discarded and washed with PBS. Biofilm fixation was done with the addition of
411 sodium acetate (2%). Crystal violet (0.1%) was used for staining followed by a final wash
412 with PBS. Absorbance at 600 nm was read using a spectrophotometer.
413
414 **DNA sequencing and genome assembly**
415 Following published protocols, genomic DNA from bacteria and phage was
416 isolated using phenol-chloroform extraction. Purified DNA was sent to Plasmidsaurus and

SeqCenter for Nanopore and Illumina sequencing, respectively. Reference genomes for bacterial strains were assembled using Flye v2.9.3 with default settings for long-reads. This resulted in 1 singular contig assemblies for 252 (2902592bp, 125x) and MW2 (2820460, 600x), and 3 contigs for LAC (2907712, 645x). Phage assemblies for Evo2 and ΦStaph1N were done with the SPADES assembler v3.15.5.

Open-reading frames (ORFs) were called on the assembled bacterial genomes using Prodigal v.2.6.3,[48] resulting in a gene-feature file (GFF), and translated genes as .faa and .fna formats. We used BLASTp (Accessed June 4th, 2024), against the protein BLAST database swissprot_2023-06-28, with an expectation value cutoff of 0.001. The top hit for each ORF was used as the final functional annotation.

**Mutation identification**

A total of 27 genomic samples were collected. DNA was extracted and sent for long-read sequencing using Oxford Nanopore Technology (Plasmidsaurus, San Francisco, USA). Reads were filtered using filtlong v0.2.1 using default settings (https://github.com/rrwick/Filtlong) and with the -p flag 95 (keeping 95% of the best reads). Quality-filtered long reads were mapped against the respective genomes using minimap2 2.22-r1101[49] resulting in 1 alignment file output per sample (.sam file). The read mapping software Minimap2[49] was selected because of its suitability to map long reads. Samtools v1.20[50] was used to convert the .sam files into .bam files, sort the bam file, index the bam files, and generate a coverage table for each position along the alignment.

Reference files (fasta and GFF files) and the 53 “sorted.bam” alignments files were imported into Geneious. Variant calling was performed using Geneious Prime Geneious Prime ® 2024.0.2 (www.geneious.com), using the custom settings: 10% coverage, minimum 95% variant frequency threshold, and the option for “Analyze effect of variants on translation” checked. Variant results and genome annotations table files were exported as a tab-separated-table, and visualized using R v4.4.0, mostly with the tidyverse package. Sequencing data processing, quality filtering, and mapping were performed at the Center for High-Throughput Computing (https://chtc.cs.wisc.edu/). BLAStp was performed on usegalaxy.eu (Accessed June 4th, 2024).

447 **Figures**

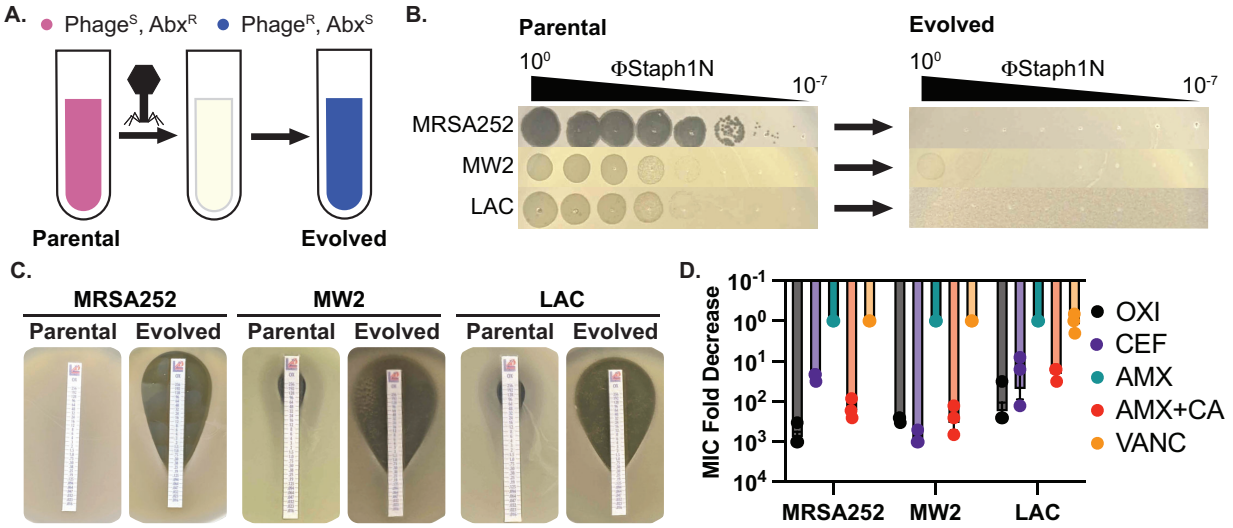


448
449

450 **Figure 1. Infection by bacteriophage ΦStaph1N drives the loss of β-lactam**
451 **resistance in MRSA. A.** Schematic of the experimental setup. Drug-resistant (Abx$^R$),
452 phage-sensitive (Phage$^S$) bacterial cultures are infected with phage. The population of
453 infected cells is passaged and allowed to recover. The surviving cell population is
454 resistant to phage infection (Phage$^R$) but has evolved sensitivity to antibiotics (Abx$^S$). **B.**
455 ΦStaph1N infects MRSA strains MRSA252, MW2, and LAC (left panel). Following
456 infection with ΦStaph1N, evolved cultures of the three MRSA strains are resistant to
457 ΦStaph1N (right panel). **C.** ΦStaph1N-treated, evolved MRSA strains show significant
458 loss of resistance against oxacillin, compared to the parental strains. Loss of resistance
459 is indicated by the area of bacterial clearance surrounding the antibiotic resistance strip.
460 **D.** ΦStaph1N treatment causes loss resistance against different β-lactams. Plotted are
461 the fold reductions of minimal inhibitory concentration (MIC) between treated and mock-
462 treated cells. OXI = oxacillin; CEF = cefazolin; AMX = amoxicillin; AMX+CA = amoxicillin
463 & clavulanic acid; VANC = vancomycin.

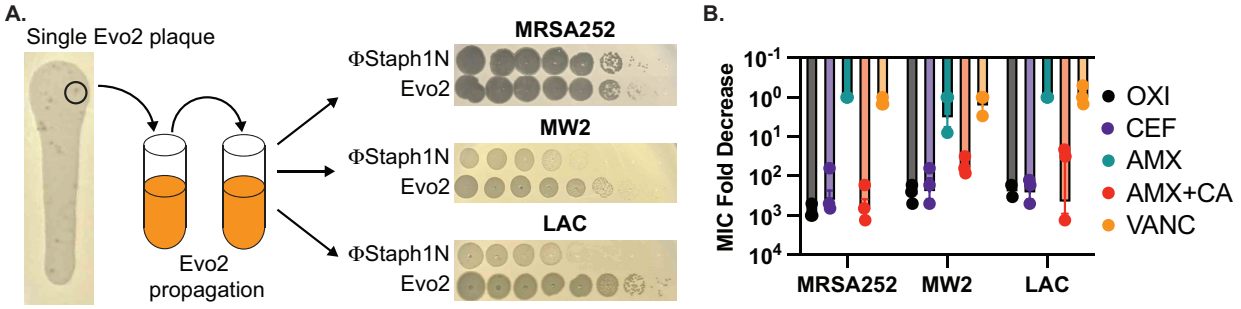


**Figure 2. Evo2 is a variant of ΦStaph1N with higher activity against MRSA**. **A.** Single Evo2 plaques appear inside hazy ΦStaph1N plaques on LAC (Left-most panel). Compared to ΦStaph1N, Evo2 shows comparable infectivity towards MRSA252 but improved infectivity towards MW2 and LAC (Right-most panels). **B.** Similar to ΦStaph1N, Evo2 infection reduces β-lactam resistance in MRSA.

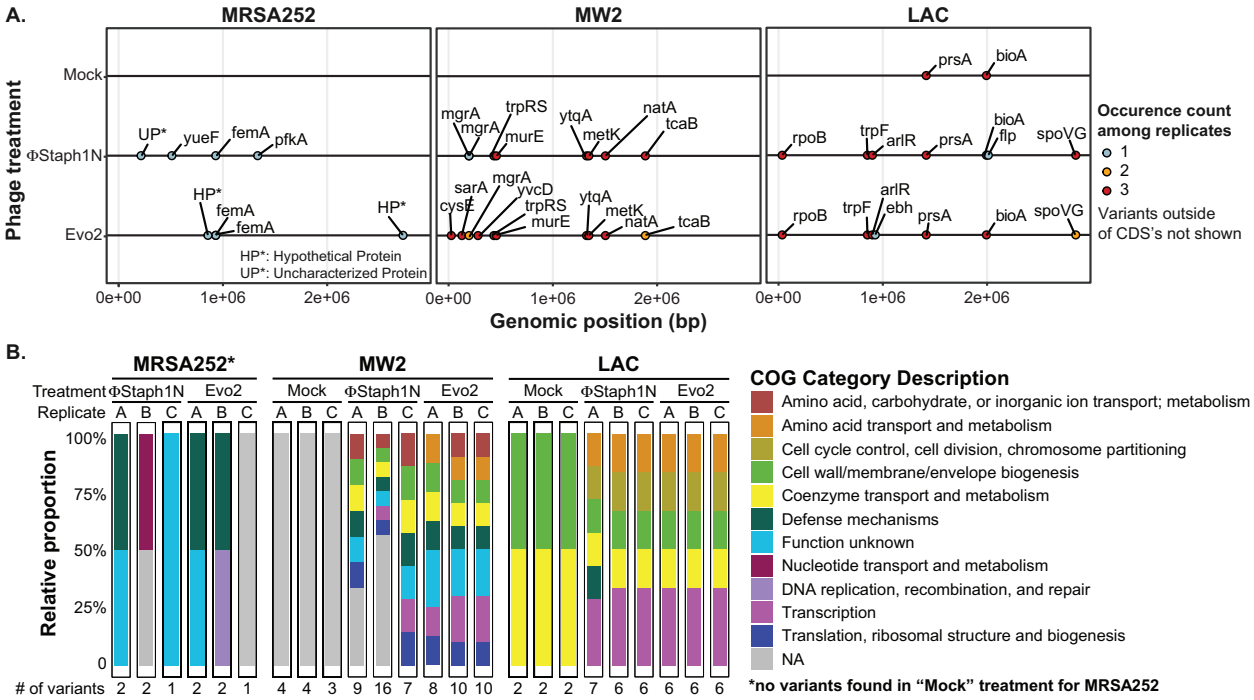


**Figure 3. Phage infection of MRSA strains produces distinct mutational profiles**. **A.** Coding sequences (CDS) with mutations from the three MRSA strains following phage treatment or mock treatment. For each strain, three isolates were sequenced and their mutations identified. Mutations are color-coded based on the number of occurrences among the three replicates. **B.** Categories of genes with mutations that arose in each MRSA strain and treatment condition.

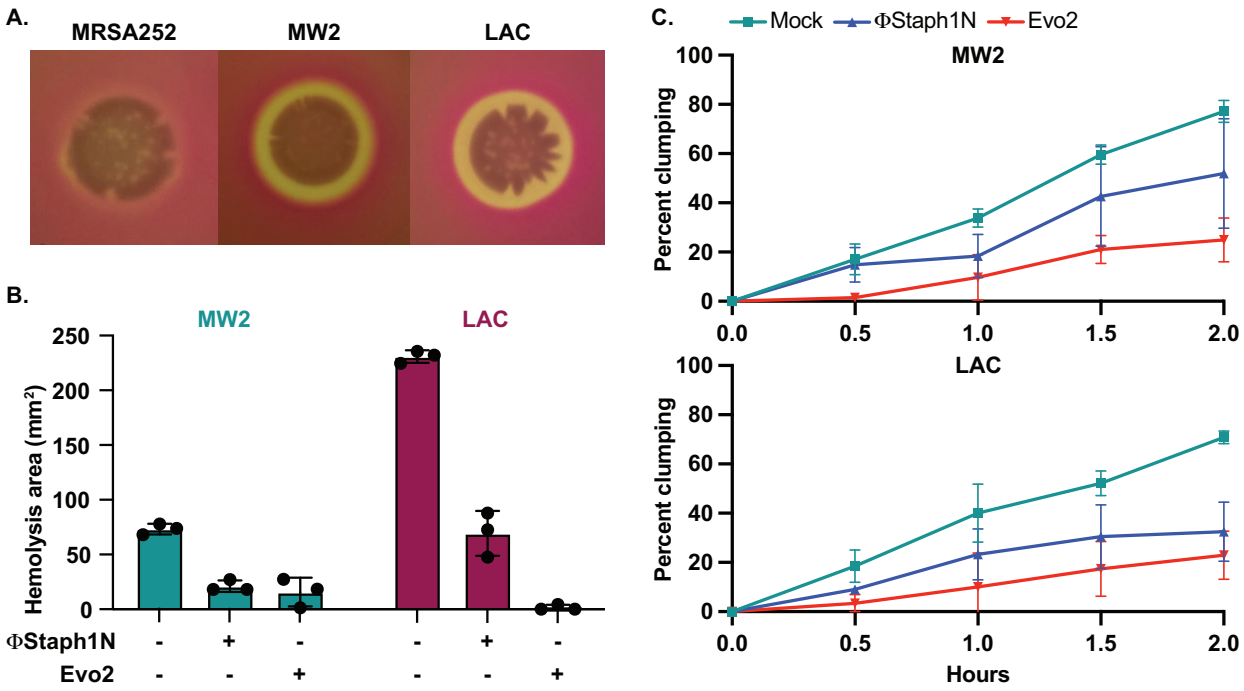


**Figure 2. Phage treatment of MRSA results in attenuated virulence phenotypes. A.** MW2 and LAC strains display hemolytic activity on rabbit blood agar plates, while MRSA252 does not. **B**. Phage-treated MW2 and LAC strains display reduced hemolysis compared to uninfected cells. **C**. Surviving cultures of MW2 and LAC treated with either ΦStaph1N (blue) or Evo2 (red) show reduced clumping rates compared to mock untreated cells (teal).

484 **Supplemental data**

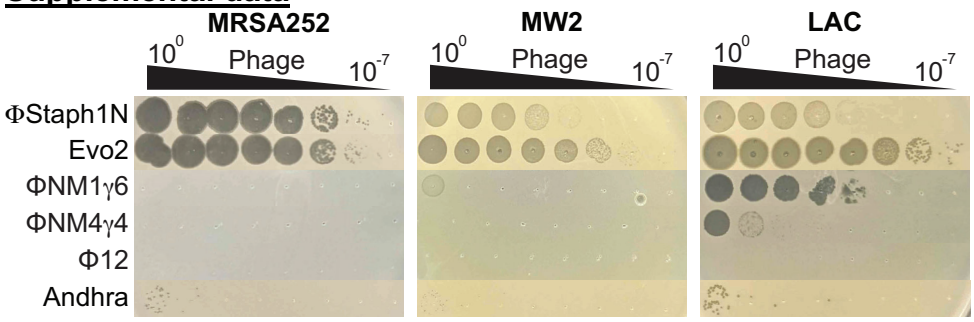


485
486
487 **Figure S1. Phage sensitivity of MRSA strains.** Efficiencies of plaquing of phages on
488 MRSA252, MW2, and LAC. Phages were 10-fold serially diluted and spotted onto top
489 agar overlays of each strain. Phage Evo2 shows the highest plaquing efficiency on all
490 three strains.

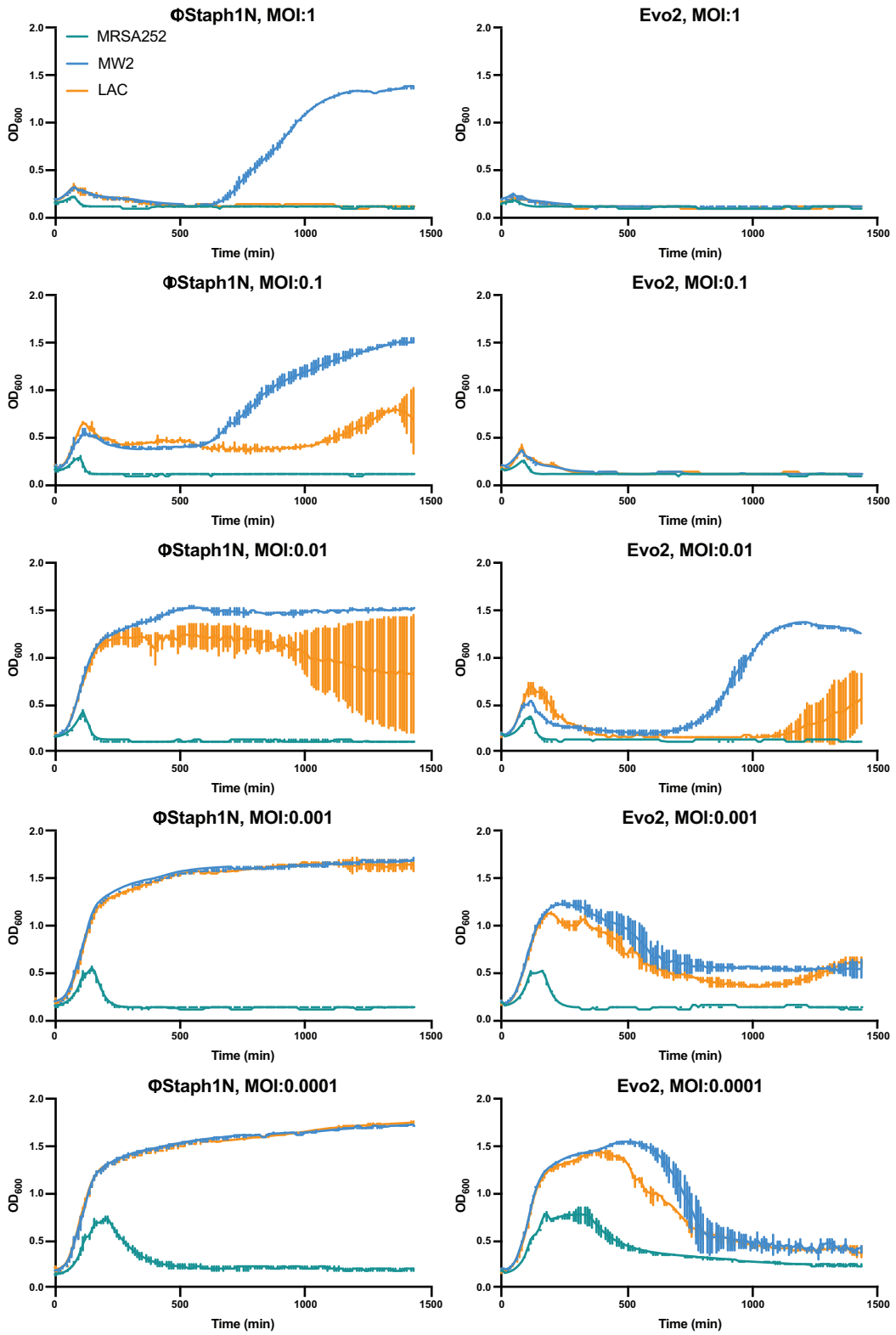


**Figure S2. Growth curves of MRSA strains under varying levels of phage infection.** MRSA252, MW2, and LAC cultures were infected with either ΦStaph1N or Evo2 at the indicated multiplicity of infection (MOI). The optical density ($OD_{600}$) of the cultures was

495 monitored on an automated plate reader. Each condition was tested in 3 independent
496 replicates.

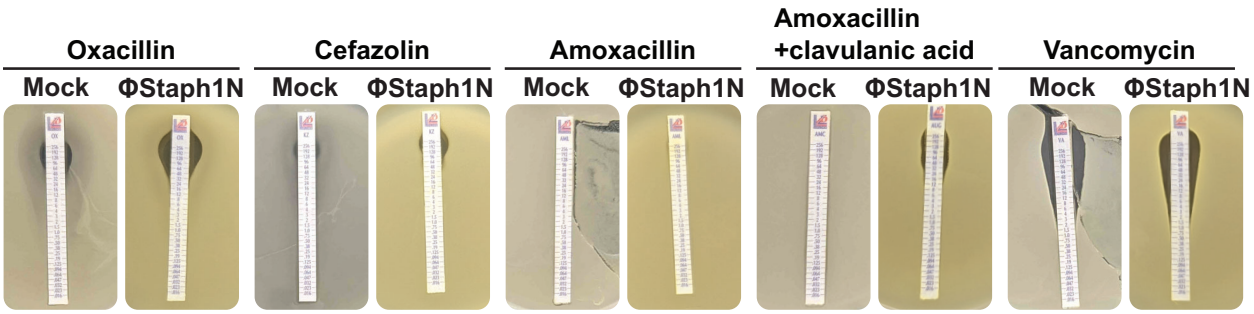


**Figure S3. Phage ΦNM1γ6 infection LAC does not drive the loss of β-lactam resistance.** LAC cultures were infected with phage at an MOI 0.1 and allowed to recover. The surviving cells were then assayed for their MICs against different β-lactams and vancomycin using antibiotic strips.

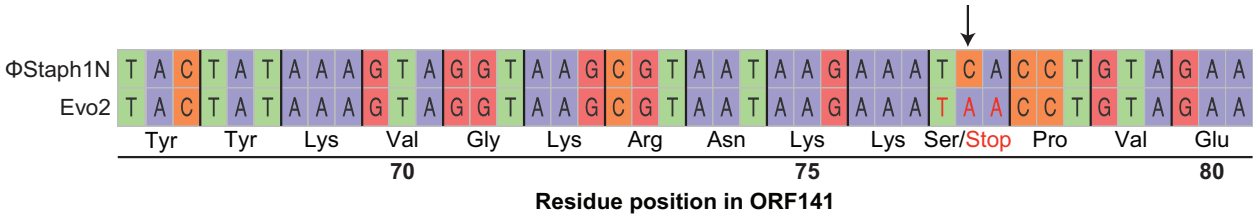


**Figure S4. Sequencing analysis of Evo2.** Evo2 is a mutant form of ΦStaph1N with a nonsense mutation in ORF141. The A to C mutation (marked by the arrow) in Evo2 converts Serine 77 of ORF141 into a stop codon.

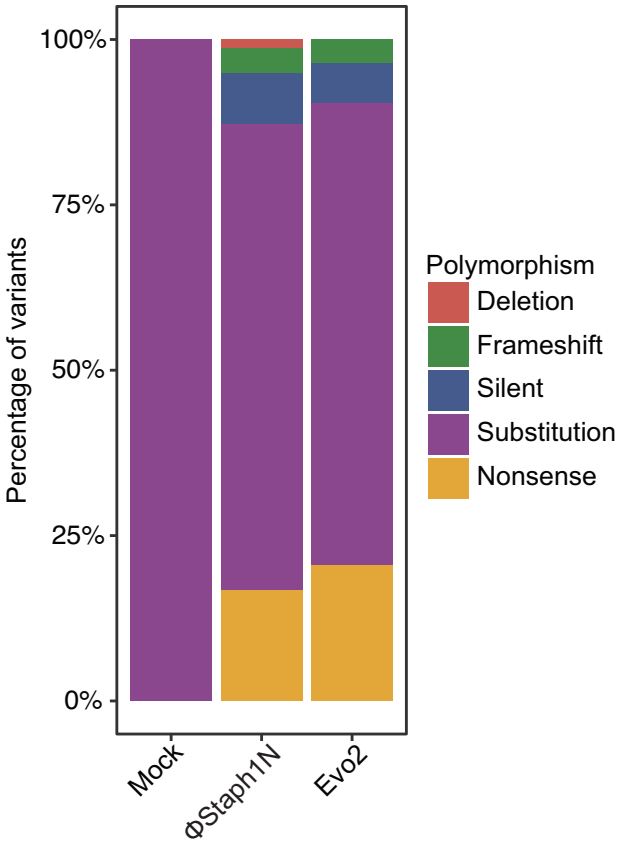


507
508 **Figure S5. Types of polymorphisms in MRSA strains following infection by phage**
509 **or a mock treatment.** Plotted are the polymorphisms that were found in a gene with an
510 assigned COG category.

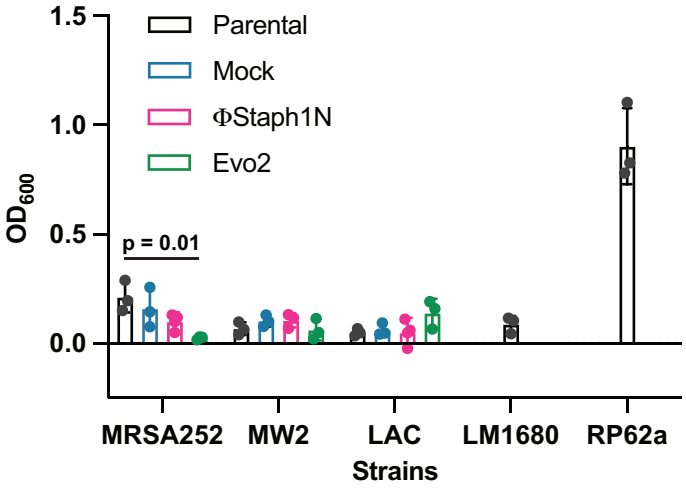


511

512 **Figure S6. Effect of phage infection on biofilm formation in MRSA strains.** Cultures
513 were infected or mock-infected with either ΦStaph1N or Evo2. RP62a is a strain of *S.*
514 *epidermidis* with known biofilm forming capability, while LM1680 is a derivative of RP62a
515 that has lost biofilm forming ability.[51,52] Biofilm biomass was assessed by staining with
516 Crystal Violet. Solubilized crystal violet was quantified by measuring absorbance at 600
517 nm. Values represent averages and standard deviations of three replicates. Statistical
518 significance was determined with a two-tailed t-test.

519 **Table S1. Bacterial strains and bacteriophages used in this study**

520

| Strain Name | Comments | Source or Reference |
|---|---|---|
| MRSA MW2 (USA400) | | Baba *et al.*, 2002 |
| MRSA LAC (USA300) | | Voyich *et al.*, 2005 |
| MRSA252 (USA200) | | Holden *et al.*, 2004 |
| *S. epidermidis* RP62a | methicillin-resistant biofilm-producing *S. epidermidis* | Christensen *et. al.*, 1982 |
| *S. epidermidis* LAM1680 | Derived from *S. epidermidis* RP62a; carries genomic deletion that inactivates biofilm production | Jiang *et al.*, 2016 |
| ΦStaph1N | | Łobocka *et al.*, 2012 |
| Evo2 | Derived from ΦStaph1N | This study |
| ΦNM1$\gamma$6 | Lytic version of ΦNM1 | Marraffini laboratory |
| ΦNM4$\gamma$4 | Lytic version of ΦNM4 | Marraffini laboratory |
| Φ12 | | Marraffini laboratory |
| Andhra | Infects *S. epidermidis* | Hatoum-Aslan laboratory |

521 **Table S2. MIC against oxacillin of MRSA strains treated with different MOIs of phage**

| | MRSA252 | | | | | |
|---|---|---|---|---|---|---|
| | Staph1N | | | Evo2 | | |
| **MOI** | **Rep 1** | **Rep 2** | **Rep 3** | **Rep 1** | **Rep 2** | **Rep 3** |
| 10^-2 | 0.25 | 0.125 | 0.38 | NG | 2 | 0.5 |
| 10^-3 | NG | 0.94 | 0.19 | 1 | 0.75 | 1 |
| 10^-4 | 0.5 | 0.25 | 0.19 | 0.75 | 1 | 0.5 |
| 10^-5 | 0.25 | 0.38 | NG | 0.38 | NG | NG |
| Mock | >256 | >256 | >256 | >256 | >256 | >256 |
| | MW2 | | | | | |
| | Staph1N | | | Evo2 | | |
| **MOI** | **Rep 1** | **Rep 2** | **Rep 3** | **Rep 1** | **Rep 2** | **Rep 3** |
| 10^-2 | 3 | 24 | 24 | 4 | NG | NG |
| 10^-3 | 32 | 24 | 48 | 4 | NG | NG |
| 10^-4 | 48 | 96 | 32 | 3 | NG | NG |
| 10^-5 | 96 | 64 | 24 | 2 | NG | NG |
| Mock | 96 | 48 | 32 | 96 | 48 | 32 |
| | LAC | | | | | |
| | Staph1N | | | Evo2 | | |
| **MOI** | **Rep 1** | **Rep 2** | **Rep 3** | **Rep 1** | **Rep 2** | **Rep 3** |
| 10^-2 | NG | NG | 2 | 0.064 | NG | NG |
| 10^-3 | NG | 3 | 1.5 | 0.032 | NG | NG |
| 10^-4 | 32 | 1.5 | 1 | NG | NG | NG |
| 10^-5 | 32 | 16 | 0.38 | NG | NG | NG |
| Mock | 32 | 48 | 48 | 32 | 48 | 48 |

522 NG: no growth detected

523

## References


1. Gorwitz, R. J. *et al.* Changes in the Prevalence of Nasal Colonization with *Staphylococcus aureus* in the United States, 2001–2004. *J INFECT DIS* **197**, 1226–1234 (2008).
2. Tomasz, A. The Mechanism of the Irreversible Antimicrobial Effects of Penicillins: How the Beta-Lactam Antibiotics Kill and Lyse Bacteria. *Annu. Rev. Microbiol.* **33**, 113–137 (1979).
3. World Health Organization. *Critically Important Antimicrobials for Human Medicine*. (World Health Organization, Geneva, 2019).
4. Zapun, A., Contreras-Martel, C. & Vernet, T. Penicillin-binding proteins and β-lactam resistance. *FEMS Microbiol Rev* **32**, 361–385 (2008).
5. Murray, C. J. L. *et al.* Global burden of bacterial antimicrobial resistance in 2019: a systematic analysis. *The Lancet* **399**, 629–655 (2022).
6. Suttle, S. W. Viruses and Nutrient Cycles in the Sea. **49**, (1999).
7. Kortright, K. E., Chan, B. K., Koff, J. L. & Turner, P. E. Phage Therapy: A Renewed Approach to Combat Antibiotic-Resistant Bacteria. *Cell Host & Microbe* **25**, 219–232 (2019).
8. Hatoum-Aslan, A. The phages of staphylococci: critical catalysts in health and disease. *Trends in Microbiology* **29**, 1117–1129 (2021).
9. Oechslin, F. Resistance Development to Bacteriophages Occurring during Bacteriophage Therapy. *Viruses* **10**, 351 (2018).
10. Azam, A. H. & Tanji, Y. Peculiarities of Staphylococcus aureus phages and their possible application in phage therapy. *Appl Microbiol Biotechnol* **103**, 4279–4289 (2019).
11. Gerlach, D. *et al.* Methicillin-resistant Staphylococcus aureus alters cell wall glycosylation to evade immunity. *Nature* **563**, 705–709 (2018).
12. Meyer, J. R. *et al.* Repeatability and Contingency in the Evolution of a Key Innovation in Phage Lambda. *Science* **335**, 428–432 (2012).
13. Bernheim, A. & Sorek, R. The pan-immune system of bacteria: antiviral defence as a community resource. *Nat Rev Microbiol* **18**, 113–119 (2020).
14. Maynard, N. D. *et al.* A Forward-Genetic Screen and Dynamic Analysis of Lambda Phage Host-Dependencies Reveals an Extensive Interaction Network and a New Anti-Viral Strategy. *PLoS Genet* **6**, e1001017 (2010).
15. Oromí-Bosch, A., Antani, J. D. & Turner, P. E. Developing Phage Therapy That Overcomes the Evolution of Bacterial Resistance. *Annu. Rev. Virol.* **10**, 503–524 (2023).
16. Berryhill, B. A., Huseby, D. L., McCall, I. C., Hughes, D. & Levin, B. R. Evaluating the potential efficacy and limitations of a phage for joint antibiotic and phage therapy of *Staphylococcus aureus* infections. *Proc. Natl. Acad. Sci. U.S.A.* **118**, e2008007118 (2021).
17. Voyich, J. M. *et al.* Insights into Mechanisms Used by *Staphylococcus aureus* to Avoid Destruction by Human Neutrophils. *The Journal of Immunology* **175**, 3907–3919 (2005).

18. Holden, M. T. G. *et al.* Complete genomes of two clinical *Staphylococcus aureus* strains: Evidence for the rapid evolution of virulence and drug resistance. *Proc. Natl. Acad. Sci. U.S.A.* **101**, 9786–9791 (2004).
19. Kobayashi, S. D. *et al.* Comparative analysis of USA300 virulence determinants in a rabbit model of skin and soft tissue infection. *J Infect Dis* **204**, 937–941 (2011).
20. Xia, G. & Wolz, C. Phages of Staphylococcus aureus and their impact on host evolution. *Infection, Genetics and Evolution* **21**, 593–601 (2014).
21. Deghorain, M. & Van Melderen, L. The Staphylococci Phages Family: An Overview. *Viruses* **4**, 3316–3335 (2012).
22. Mo, C. Y. *et al.* Type III-A CRISPR immunity promotes mutagenesis of staphylococci. *Nature* **592**, 611–615 (2021).
23. Goldberg, G. W., Jiang, W., Bikard, D. & Marraffini, L. A. Conditional tolerance of temperate phages via transcription-dependent CRISPR-Cas targeting. *Nature* **514**, 633–637 (2014).
24. Baba, T., Bae, T., Schneewind, O., Takeuchi, F. & Hiramatsu, K. Genome Sequence of *Staphylococcus aureus* Strain Newman and Comparative Analysis of Staphylococcal Genomes: Polymorphism and Evolution of Two Major Pathogenicity Islands. *J Bacteriol* **190**, 300–310 (2008).
25. Li, L. *et al.* The Global Regulon *sarA* Regulates β-Lactam Antibiotic Resistance in Methicillin-Resistant *Staphylococcus aureus* In Vitro and in Endovascular Infections. *J Infect Dis.* **214**, 1421–1429 (2016).
26. Zielinska, A. K. *et al.* *SARA* -mediated repression of protease production plays a key role in the pathogenesis of *S taphylococcus aureus* USA 300 isolates. *Molecular Microbiology* **86**, 1183–1196 (2012).
27. Crosby, H. A. *et al.* The Staphylococcus aureus Global Regulator MgrA Modulates Clumping and Virulence by Controlling Surface Protein Expression. *PLoS Pathog* **12**, e1005604 (2016).
28. Kwiecinski, J. M. *et al.* Staphylococcus aureus uses the ArlRS and MgrA cascade to regulate immune evasion during skin infection. *Cell Reports* **36**, 109462 (2021).
29. Panchal, V. V. *et al.* Evolving MRSA: High-level β-lactam resistance in Staphylococcus aureus is associated with RNA Polymerase alterations and fine tuning of gene expression. *PLoS Pathog* **16**, e1008672 (2020).
30. Bai, J. *et al.* The role of ArlRS in regulating oxacillin susceptibility in methicillin-resistant *Staphylococcus aureus* indicates it is a potential target for antimicrobial resistance breakers. *Emerging Microbes & Infections* **8**, 503–515 (2019).
31. Walker, J. N. *et al.* The Staphylococcus aureus ArlRS Two-Component System Is a Novel Regulator of Agglutination and Pathogenesis. *PLoS Pathog* **9**, e1003819 (2013).
32. Schulthess, B. *et al.* The $\sigma^B$ -Dependent *yabJ-spoVG* Operon Is Involved in the Regulation of Extracellular Nuclease, Lipase, and Protease Expression in Staphylococcus aureus. *J Bacteriol* **193**, 4954–4962 (2011).
33. Liu, X., Zhang, S. & Sun, B. SpoVG Regulates Cell Wall Metabolism and Oxacillin Resistance in Methicillin-Resistant Staphylococcus aureus Strain N315. *Antimicrob Agents Chemother* **60**, 3455–3461 (2016).

611 34. Chen, C. *et al.* Characterization of serine acetyltransferase (CysE) from methicillin-
612 resistant Staphylococcus aureus and inhibitory effect of two natural products on
613 CysE. *Microbial Pathogenesis* **131**, 218–226 (2019).
614 35. Markham, G. D., DeParasis, J. & Gatmaitan, J. The sequence of metK, the structural
615 gene for S-adenosylmethionine synthetase in Escherichia coli. *Journal of Biological*
616 *Chemistry* **259**, 14505–14507 (1984).
617 36. Proctor, A. R. & Kloos, W. E. Tryptophan Biosynthetic Enzymes of *Staphylococcus*
618 *aureus*. *J Bacteriol* **114**, 169–177 (1973).
619 37. Maidhof, H., Reinicke, B., Blümel, P., Berger-Bächi, B. & Labischinski, H. femA,
620 which encodes a factor essential for expression of methicillin resistance, affects
621 glycine content of peptidoglycan in methicillin-resistant and methicillin-susceptible
622 Staphylococcus aureus strains. *J Bacteriol* **173**, 3507–3513 (1991).
623 38. Srisuknimit, V., Qiao, Y., Schaefer, K., Kahne, D. & Walker, S. Peptidoglycan Cross-
624 Linking Preferences of Staphylococcus aureus Penicillin-Binding Proteins Have
625 Implications for Treating MRSA Infections. *J. Am. Chem. Soc.* **139**, 9791–9794
626 (2017).
627 39. Gardete, S. *et al.* Role of *murE* in the Expression of β-Lactam Antibiotic Resistance
628 in *Staphylococcus aureus*. *J Bacteriol* **186**, 1705–1713 (2004).
629 40. Jaroch, M. *et al.* Alternate routes to mnm $^{5}$ s $^{2}$ U synthesis in Gram-positive bacteria.
630 *J Bacteriol* **206**, e00452-23 (2024).
631 41. Kobayashi, K. *et al.* Comprehensive DNA Microarray Analysis of *Bacillus subtilis*
632 Two-Component Regulatory Systems. *J Bacteriol* **183**, 7365–7370 (2001).
633 42. Maki, H., McCallum, N., Bischoff, M., Wada, A. & Berger-Bächi, B. *tcaA* Inactivation
634 Increases Glycopeptide Resistance in *Staphylococcus aureus*. *Antimicrob Agents*
635 *Chemother* **48**, 1953–1959 (2004).
636 43. Otto, M. Staphylococcus aureus toxins. *Current Opinion in Microbiology* **17**, 32–37
637 (2014).
638 44. Jurado, A., Fernández, L., Rodríguez, A. & García, P. Understanding the
639 Mechanisms That Drive Phage Resistance in Staphylococci to Prevent Phage
640 Therapy Failure. *Viruses* **14**, 1061 (2022).
641 45. Moller, A. G. *et al.* Genes Influencing Phage Host Range in Staphylococcus aureus
642 on a Species-Wide Scale. **6**, (2021).
643 46. Crosby, H. A., Kwiecinski, J. M. & Horswill, A. R. In Vitro Assay for Quantifying
644 Clumping of Staphylococcus aureus. in *Staphylococcus aureus* (ed. Rice, K. C.) vol.
645 2341 31–36 (Springer US, New York, NY, 2021).
646 47. Feoktistova, M., Geserick, P. & Leverkus, M. Crystal Violet Assay for Determining
647 Viability of Cultured Cells. *Cold Spring Harb Protoc* **2016**, pdb.prot087379 (2016).
648 48. Hyatt, D. *et al.* Prodigal: prokaryotic gene recognition and translation initiation site
649 identification. *BMC Bioinformatics* **11**, 119 (2010).
650 49. Li, H. Minimap2: pairwise alignment for nucleotide sequences. *Bioinformatics* **34**,
651 3094–3100 (2018).
652 50. Li, H. *et al.* The Sequence Alignment/Map format and SAMtools. *Bioinformatics* **25**,
653 2078–2079 (2009).
654 51. Christensen, G. D., Simpson, W. A., Bisno, A. L. & Beachey, E. H. Adherence of
655 slime-producing strains of Staphylococcus epidermidis to smooth surfaces. *Infect*
656 *Immun* **37**, 318–326 (1982).

657 52. Jiang, W. *et al.* Dealing with the Evolutionary Downside of CRISPR Immunity:
658 Bacteria and Beneficial Plasmids. *PLoS Genet* **9**, e1003844 (2013).
659